2026 IEEE International Conference on Robotics and Automation (ICRA 2026)
June 1-5, 2026. Vienna, Austria

Shared Haptic Control for Surgical Skill Transfer on a Dual-Console da Vinci Research Kit

Xiangyi Le[1*], Nan Jiang[2*], Pucheng Shao[1*], Brendan Burkhart[1], Peter Kazanzides[1,2], Ugur Tumerdem[1,3]

***Abstract*— Robotic surgery has revolutionized minimally invasive procedures by offering enhanced precision, dexterity, and patient outcomes. However, the training and operational paradigms in robotic surgery have not evolved in parallel. Current apprenticeship models fall short in this domain, as robotic surgery isolates the primary surgeon in a teleoperated control loop, limiting opportunities for hands-on learning by trainees. To address this, we present the first implementation of a multilateral controller on a da Vinci Research Kit (dVRK), enabled by a four-channel teleoperation architecture and learning-based force estimation on a dual-console setup. This framework allows an expert and novice to share motion and force authority on the patient side robots through an adjustable dominance factor. We validated the system in three experiments. In transparency tests, the architecture achieved sub-millimeter position tracking errors (PTE $\leq$ 0.2 mm) and force tracking errors (FTE $\leq$ 1 N). In a palpation pilot user study (N=10) with tumor-tissue phantoms, participants identified stiffer regions, without visual feedback, with 83% accuracy in single-user mode (α = 1) and 74% accuracy in dual-user shared mode (α = 0.5). In a suturing force control pilot user study (N=10), novices significantly reduced force error and increased time within the safe range after expert-guided training, with no suture breakage observed post-training. These results on a dual-console dVRK setup demonstrate the feasibility of expert-in-the-loop training with real-time haptic guidance, positioning multilateral teleoperation as a promising approach for surgical skill transfer.**

I. INTRODUCTION

Robotic-assisted minimally invasive surgery (RAMIS) has transformed clinical practice by enhancing dexterity, precision, and ergonomics. Among RAMIS platforms, the da Vinci Surgical System (Intuitive Surgical Inc., Sunnyvale, CA) is the most widely adopted, with thousands of installations worldwide [1]. Despite their success, commercial systems mostly lack haptic feedback (with the latest da Vinci 5 [2] being one exception), depriving surgeons of force and tactile cues that are fundamental for safe and effective tissue manipulation [3]. This limitation not only impacts expert performance but also presents challenges for surgical training, where force misapplication can lead to tissue damage or poor skill acquisition.

Research over the past two decades has sought to restore haptic feedback in robotic surgery through sensorized instruments [4]–[7] and sensorless force estimation [3], [8]–[10]. Bilateral teleoperation with haptic feedback has been studied extensively in both surgical and non-surgical contexts, showing that transparency, often defined as accurate position and force tracking between master and follower, is critical for operator performance [11]–[14]. However, nearly all of these studies consider bilateral teleoperation with a master and a follower robot.

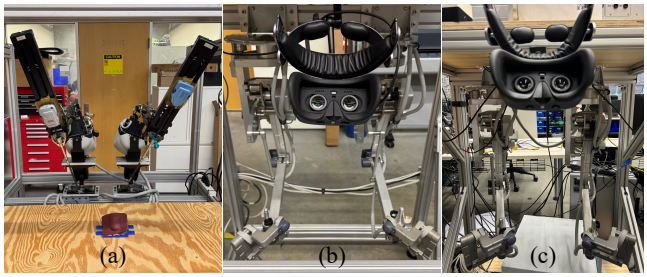

Fig. 1. A Dual-Console da Vinci Research Kit. a) Patient Side Manipulators (PSMs); b) Novice Console and Master Tool Manipulators (MTMs); c) Expert Console and Master Tool Manipulators

Despite the advantages of robotic surgery over conventional laparoscopy, training with current robotic surgery systems, as critically examined by Beane [15], can often fail to produce surgeons with adequate hands-on training experience in the operating room. Residents are frequently relegated to passive observation to ensure patient safety. While this model is necessary for risk management, it prevents the active, hands-on experience required to develop critical motor skills and adaptive decision-making.

Robotic surgery vendors have introduced virtual reality (VR) simulators to offer risk-free practice of basic tasks [16]; however, systematic reviews [17], [18] indicate that while these systems enhance fundamental technical skills, they often fail to capture the complexity of real procedures needed for advanced surgical competencies. Complementary strategies integrating haptic and visual guidance [19], [20] and motion replay methods [21] can improve performance, though the "guidance hypothesis" warns that excessive support might impede autonomous skill development.

In surgical education, dual-console systems [22] (such as the da Vinci Xi dual-console) are increasingly used for mentoring, allowing an expert to take over control from a trainee. Yet, current implementations are limited to switching or splitting control rather than dynamically sharing control authority through kinesthetic coupling with haptic feedback. Recent proposals for multi-user multilateral haptic training systems [23]–[28] promise more intuitive, real-time haptic feedback by dynamically adjusting control authority between users for shared control, yet such systems have not been fully

[1] LCSR, [2]Dept. of Computer Science, Johns Hopkins University, Baltimore, MD 21218, USA (email: xle6@jh.edu)
[3]Dept. of Mechanical Engineering, Marmara University, Istanbul, Turkey
*These authors contributed equally to this work.

realized on clinical platforms due to challenges in obtaining reliable haptic measurements. To our knowledge, there is no prior demonstration of multilateral haptic shared control on a da Vinci platform.

Contributions: This paper presents the first implementation and feasibility demonstration of multilateral haptic teleoperation on a da Vinci system (dVRK) [29]. This is achieved through our novel framework with learning based sensorless force estimation and a four channel (position and force exchange) multilateral teleoperation architecture. Our framework enables multiple operators (expert and novice) to share control authority through adjustable dominance factors.

We evaluate the system through three sets of experiments:

1) Transparency: assessment of position and force tracking under the proposed transparency optimized four-channel control architecture.
2) Tumor detection through palpation: a pilot user study evaluation of force perception and performance across different dominance factor allocations, providing insights into optimal strategies for haptic shared-control.
3) Suturing force control: a pilot user study where novices are guided by an expert in applying correct suture forces, demonstrating the potential for hands-on surgical training.

By bridging shared control and haptic teleoperation for surgical training, and introducing a dual-console da Vinci Research Kit for the first time, this work establishes multilateral shared haptic control as a promising paradigm for surgical education and cooperative skill transfer.

II. METHOD

To enhance hands-on training in robotic surgery, we propose a multilateral teleoperation framework implemented on a da Vinci Research Kit (dVRK) system with dual-consoles (Fig. 1). In a typical da Vinci Surgical System, a surgeon operates from a console equipped with two master tool manipulators (MTMs), footpedals for clutching and endoscope control, and a stereo display that provides detailed views from the endoscopic camera. The surgeon controls the MTMs with both hands, and the corresponding patient-side manipulators (PSMs) replicate these scaled-down motions. In the standard unilateral teleoperation framework, the MTMs serve as masters and the PSMs as followers, with no kinesthetic (position/force) feedback transmitted from the PSMs back to the MTMs.

With the proposed dual-console dVRK system as shown in Fig. 2, two surgeons can simultaneously teleoperate the same PSMs. The right-hand MTMs are coupled with the right-hand PSM and the left-hand MTMs with the left-hand PSM, forming a multilateral teleoperation loop that incorporates both position and force feedback between the PSMs and MTMs. Control authority over each PSM is governed by dominance factors defined within the multilateral control law.

A. Teleoperation Architecture of Dual-Console dVRK system

To achieve transparency in bilateral teleoperation [11], Lawrence [12] showed that it is necessary to exchange

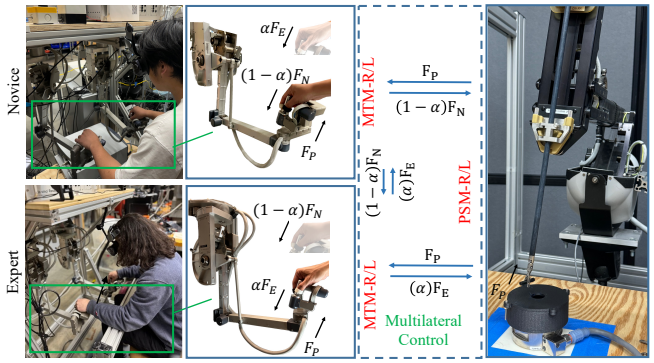

Fig. 2. Haptic Shared Control on a dual-console dVRK through multilateral teleoperation. α is the dominance factor, F_E, F_N, F_P are the expert, novice and patient side robot forces. The right MTMs control the right PSM and the left MTMs control the left PSM. Position control and motion/force scalings have been omitted for clarity.

both position and force measurements between the master and follower robots, and proposed the four-channel control architecture. This framework was later extended to multi-user multilateral teleoperation systems for haptic training [23], [24], [27]. Inspired by these works, we introduce a four-channel teleoperation architecture for the dual-console dVRK for optimized system transparency in multilateral teleoperation. To address authority allocation between the expert and the novice for haptic training, we introduce a single dominance factor $0 \leq \alpha \leq 1$. To address the motion and force scaling typically required between the MTMs and PSMs in robotic surgery, we introduce a position scaling factor β and a force scaling factor γ. These terms allow hand motions and forces at the master console to be appropriately scaled down on the patient side.

Based on this formulation, we propose the following control law for the left-hand manipulators coupling the Expert MTM-L, the Novice MTM-L, and the PSM-L. An identical controller is applied to the right-hand manipulators, linking Expert MTM-R, Novice MTM-R, and PSM-R:

$$\begin{aligned} F_{cP} &= C_p(\alpha X_E + (1-\alpha)X_N - \beta X_P) \\ &\quad + C_f(\alpha \hat{F}_E + (1-\alpha)\hat{F}_N + \gamma \hat{F}_P) \qquad (1) \\ F_{cE} &= C_p(\beta X_P - X_E) \\ &\quad + C_f(\alpha \hat{F}_E + (1-\alpha)\hat{F}_N + \gamma \hat{F}_P) \qquad (2) \\ F_{cN} &= C_p(\beta X_P - X_N) \\ &\quad + C_f(\alpha \hat{F}_E + (1-\alpha)\hat{F}_N + \gamma \hat{F}_P) \qquad (3) \end{aligned}$$

where F_{cE}, F_{cN}, F_{cP} denote controller forces of the Expert MTM, the Novice MTM and the corresponding PSM, respectively, and $\hat{F}_E$, $\hat{F}_N$, and $\hat{F}_P$ are the estimated external forces applied to the corresponding components. C_p is the control gain of a position-channel PD controller and C_f is the control gain of a force-channel proportional controller. Together, they constitute the controller of a robot arm, and each robot arm is equipped with an independent controller. Note that while the teleoperation framework is constructed in Cartesian space, the underlying low-level controllers are

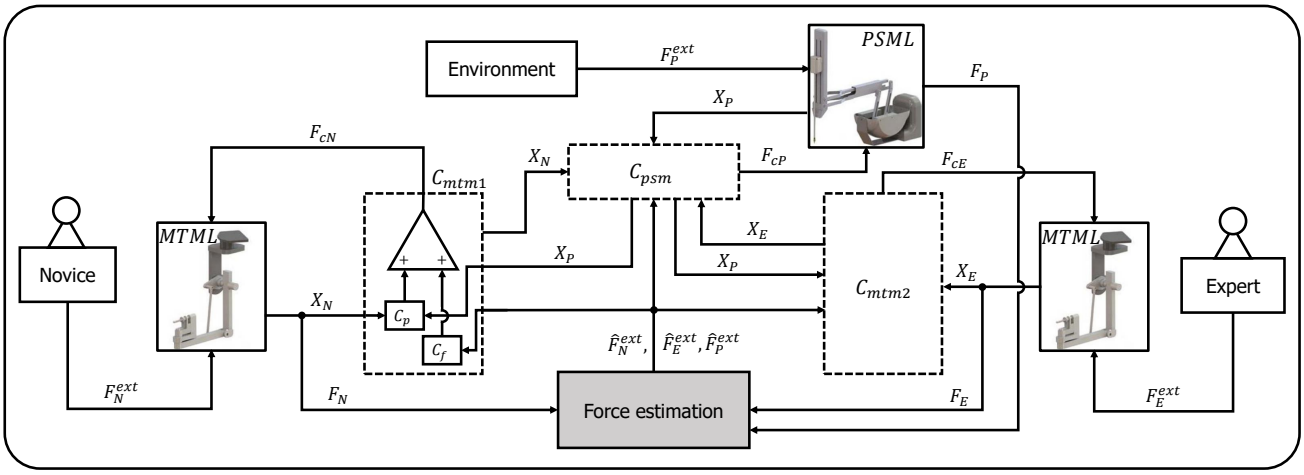

Fig. 3. Control block diagram for the left hand of the dual-console dVRK. The other hand follows the same control architecture. The three dashed boxes denote the robot arm controllers of identical structure, each comprising a position and a force controller. The force estimation module is described in Subsection: Learning-Based External Force Estimation.

in joint space. The software performs the necessary transformations between the two spaces. The control block diagram is illustrated in Fig. 3.

This control law is formulated to satisfy the following transparency relations between robot forces and velocities, assuming ideal conditions such as perfect dynamic compensation and negligible communication delays:

$$\begin{bmatrix} \dot{X}_E \\ \dot{X}_N \\ F_P \end{bmatrix} = \underbrace{\begin{bmatrix} 0 & 0 & -\beta \\ 0 & 0 & -\beta \\ -\alpha/\gamma & -(1-\alpha)/\gamma & 0 \end{bmatrix}}_{G_{mod}} \begin{bmatrix} F_E \\ F_N \\ -\dot{X}_P \end{bmatrix} \tag{4}$$

where G_{mod} is the modified inverse hybrid matrix [27].

Under this condition, the proposed control law ensures that the MTMs move together and that the PSM follows their scaled motion: $\alpha X_E + (1-\alpha)X_N = \beta X_P$. The master forces will be transmitted to each other and to the PSM as determined by the dominance factor selection: $\alpha F_E + (1-\alpha)F_N = -\gamma F_P$. The users will move the same PSM instrument together and will therefore feel the forces from each other as well as from the environment (in opposite direction).

B. Dominance Factor setting for Multilateral Shared Control

In multilateral teleoperation, each operator's influence on the follower can be adjusted using dominance factors, which weight the contributions of their commands. By tuning these parameters, the system can be switched between guidance, training, and evaluation modes within a haptic training curriculum [25].

In our framework, we employ a single dominance factor α. When $\alpha = 0$ or 1, the system reduces to a bilateral teleoperation loop between one user and the PSM, while the second user passively follows the motion and perceives haptic feedback without contributing input. These configurations correspond to the evaluation and guidance modes respectively. In guidance mode the novice follows the expert motion to obtain muscle memory, whereas in evaluation mode the expert can evaluate stand-alone novice performance. When $0 < \alpha < 1$, the system operates in training mode, where both users contribute motion goals to the PSM with relative influence determined by α. While some studies assign separate dominance factors to position and force channels [27], we apply a shared factor for both, providing a unified measure of each user's influence.

It should be noted that in our case, α is omitted from the master position goals in Eq. 2 and Eq. 3. The reason is that including it in the control law (e.g., $C_p(\beta X_P - \alpha X_E)$ would lead to singularities in the controller goals when $\alpha = 0/1$.

C. Learning-Based External Force Estimation

External forces can be estimated from joint torques [10]. In the dVRK, joint torques are computed by measuring the motor currents and converting them through the motor torque constants. One limitation of this approach is that the measured joint torques are the sum of the internal (dynamics) torques required to move the robot and the external torques due to contact with the environment. For precise haptic feedback from the environment, it is desirable to subtract the dynamics torques (which include the effect of gravity) from the total measured torque.

One way to achieve this is by identifying robot dynamics with neural networks. Following our previous works [10], [14], [30], we build a network consisting of a long short-term memory (LSTM) layer and three fully connected (FC) layers. Each network is responsible for the identification of three robot joints. The model's inputs are the joint positions and velocities, and its outputs are the estimated internal joint torques. We compute estimated internal Cartesian forces from the identified internal joint torques and subtract them from the measured total Cartesian forces to obtain the external force. Fig. 4 shows our pipeline for force estimation. In our dual-console dVRK system, six robots (four MTMs and two PSMs) are used, meaning that twelve models are

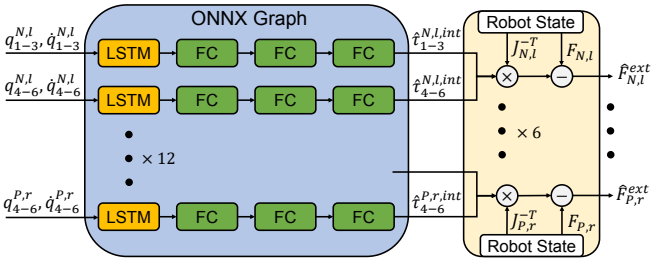

Fig. 4. Force estimation pipeline. (l and r indicates the left and right hand of the console.)

executed during each control loop. Having smaller networks improves identification performance, but a large number of models, in our case, introduces significant latency. To address latency, we merge all models into a single graph by the Open Neural Network Exchange (ONNX) library. This graph can be optimized by ONNX graph optimization, and thus reduce the computational cost associated with redundant activation of identical model structures.

D. Hardware Setup and Software Implementation

Figure 5 presents a block diagram of the system implementation. A standard dVRK, consisting of two MTMs and two PSMs, is designed for single-user operation. To enable dual-user operation, one dVRK console is connected to the control PC via FireWire (IO1), while two additional MTMs from a second console are integrated into the system through an Ethernet connection (IO2). All robot arms are teleoperated within a single Python executable, and all the data related to robot states, robot motion commands, identification of the second console, as well as the communication between the two dVRK consoles, are managed by the dVRK system component [29]. Note that the Python code directly interfaces with the C++ dVRK system component, avoiding overhead due to middleware such as ROS.

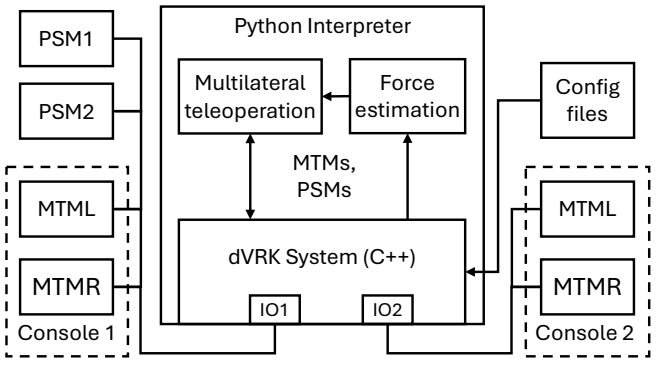

Fig. 5. Software block diagram. Standard dVRK system component (C++) is loaded as Python module and configured to use two I/O ports to communicate with arms (MTMs, PSMs) and footpedals (not shown). Multilateral teleoperation and force estimation are implemented as Python threads and interface to arm Cartesian and joint controllers, respectively, in dVRK system component.

The software is implemented in Python using a pseudo-dual-thread architecture. The main thread runs the teleoperation control loop at 850 Hz, handling tasks such as robot arm alignment, state query, and controller execution, while a secondary thread periodically performs model inference for force estimation at 300 Hz. During each control loop, external force commands are taken from the models' outputs. If there are no new results from the models, the controller maintains the most recent output.

III. Experiment Design

To evaluate the performance of our system, we conducted three experiments, divided into two major categories: (A) quantitative evaluation of transparency through force tracking and position tracking; and (B) user studies consisting of a palpation test and a suture pulling test. The two user studies, each with 10 novice (non-medical) subjects, were approved by our institutional review board (HIRB 00000701) and focused on assessing the performance of shared haptic feedback and the feasibility of surgical skill transfer. In the experiments, β in eq. 1 is set to 5 for safety, meaning that the motion of the PSM is scaled down by a factor of 5 with respect to the users' motion on the MTMs. This reduction in effective motion amplitude also helps mitigate hand tremors. In addition, the peak output torques of the PSMs and MTMs in the dVRK are different. We observed peak MTM forces around 5 N and PSM forces around 7 N, so we set γ to 0.7 to match saturation thresholds.

A. System Transparency Evaluation

In this experiment, the dual-console dVRK system was operated by two users in training mode, with the dominance factor set to $\alpha = 0.5$. The shared control tasks, including free motion and contact with rigid objects, were designed to evaluate system transparency in both the position and force channels. In the free motion task, each of the two operators manipulated their MTMs to execute a specific trajectory, while their three-dimensional Cartesian positions were recorded throughout the task. In the object contact task, a 3D printed hard platform was fixed to the workbench, as illustrated in Fig. 6(a-c). The two operators were asked to press the platform sequentially and then simultaneously. The pressing task comprised three trials in total, each along a different axis (X, Y, and Z), with force data, measured from robot arms, recorded for each trial. All tasks were performed separately for each hand.

Position tracking ability was quantified by the Position Tracking Error (PTE), which is the difference between the weighted MTM positions and the PSM position. Similarly, the Force Tracking Error (FTE) was computed as the difference between the weighted MTM forces and the PSM force, representing the force-matching performance. Following the transparency matrix (4), the errors are given by:

$$PTE = \alpha X_E + (1-\alpha)X_N - \beta X_P \tag{5}$$

$$FTE = \alpha \hat{F}_E + (1-\alpha)\hat{F}_N + \gamma \hat{F}_P \tag{6}$$

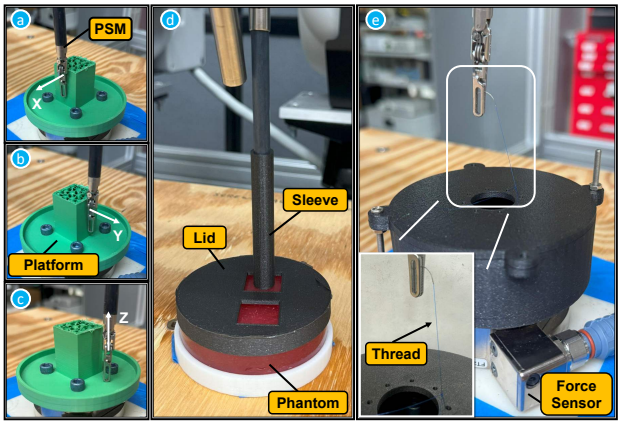

Fig. 6. Experiment setup for contact test, contact in (a) X-axis, (b) Y-axis, (c) Z-axis, (d) palpation test and (e) suture pulling test.

We used the root mean square error (RMSE) and the normalized root mean square error (NRMSE) for position and force tracking evaluations. RMSE is defined as

$$\text{RMSE} = \sqrt{\frac{1}{N}\sum_{i=1}^{N}(y_i - \hat{y}_i)^2} \tag{7}$$

NRMSE is defined as

$$\text{NRMSE} = \frac{\text{RMSE}}{y_{\max} - y_{\min}} \tag{8}$$

For position tracking, y_i corresponds to the measured PSM trajectory and $\hat{y}_i$ to the combined MTMs trajectory. For force tracking, y_i corresponds to the measured PSM force and $\hat{y}_i$ corresponds to the combined MTMs force.

B. User Study 1: Palpation

This experiment evaluates whether force feedback from the PSMs, within a shared-control framework, enables users to distinguish differences in tissue stiffness, thereby highlighting its potential value in clinical training. For this purpose, two tissue phantoms were prepared. Specifically, Phantom 1 (100 mL plastisol + 50 mL softener) and Phantom 2 (150 mL plastisol) were selected as representative samples. Tumor phantoms, composed of 100 mL plastisol and 100 mL hardener, were embedded into the tissue phantoms during the molding process. This provides two phantoms of different stiffness contrast levels: Phantom 1 has a large stiffness contrast (1500 vs. 450 N/m), whereas Phantom 2 has a small stiffness contrast (3000 vs. 2600 N/m). The experiment setup is shown in Fig. 6(d). A rigid sleeve was fitted onto the PSM end effector to prevent potential damage to the phantom without compromising haptic feedback. Additionally, to eliminate visual bias, the phantom was occluded by a 3D-printed lid, leaving only two openings for palpation, one of which concealed a tumor. The initial palpation region was randomly assigned at the beginning of each trial.

All ten participants took part in the palpation experiment, which consists of two stages: a single-user stage and a dual-user stage. In the single-user stage, each participant completed five trials, with each trial consisting of four palpation attempts under $\alpha = 1$. In the dual-user stage, the ten participants were divided into five groups of two, and each group performed five trials under $\alpha = 0.5$, where the two participants alternated palpation for four attempts and then submitted their answers simultaneously. After each trial, the participants were asked to identify the region with tumor, and their answers were recorded for analysis.

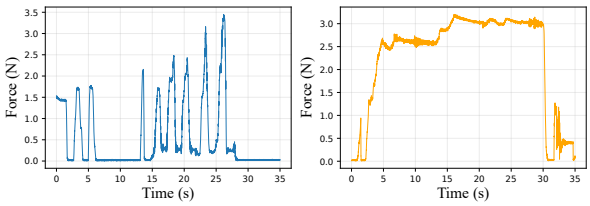

Fig. 7. Force-time curve measured from a force sensor during dual-user palpation test (left) and suture pulling test (right), illustrating the user's interaction behavior

As a representative example, Fig. 7 (left) shows the force-time curve during one dual-user palpation trial, demonstrating the characteristic interaction of participants.

C. User Study 2: Suture pulling

In the third experiment, we designed a suturing force control case using a 3D printed platform fixed to a force/torque sensor. A suture thread (size 5-0) was fixed to the platform with a surgical knot, and only one PSM was required to pull the thread to achieve the desired suturing tension. In Fig. 6(e), the setup for this experiment is illustrated, and the thread and knot can be seen in the lower left corner. The setting of the dominance factor is $\alpha = 0.5$ during the experiments. Each participant sequentially completed the following five phases in one session:

i One standalone trial as baseline: participants were instructed to pull the suture for approximately 30 seconds.

ii Three training trials: while participants pulled the suture, an operator monitored the force magnitude from the force sensor and gave corrective haptic guidance, assisting the participant to keep the force magnitude between a predefined range for approximately 30 seconds. Based on the maximum suturing force reported in [31], we defined the ideal surgical suturing force range between [2.5, 4.5] N. To avoid bias from force monitoring, only the operator was able to view the force magnitude plot. It should be noted that none of the participants had prior robotic suturing experience and the force sensor was used to emulate an expert's judgment of appropriate force during suturing.

iii One post-training trial: participants were asked to pull the suture for approximately 30 seconds without guidance. As a representative example, Fig. 7 (right) shows the force-time curve during one suture pulling trial, demonstrating the characteristic interaction of participants.

The complete procedure ensures that all participants experienced the full training process, and we compared the

TABLE I

RMSE AND NRMSE (%) OF POSITION TRACKING (FREE MOTION) AND FORCE TRACKING (PRESSING TASK).

	Position RMSE (mm)			**Position NRMSE (%)**			**Force RMSE (N)**			**Force NRMSE (%)**		
Axes	X	Y	Z	X	Y	Z	X	Y	Z	X	Y	Z
Left hand	0.11	0.17	0.09	0.20	0.42	0.21	0.59	0.64	0.67	5.53	7.65	9.42
Right hand	0.12	0.17	0.17	0.19	0.53	0.24	0.65	0.62	0.83	9.65	9.00	9.93

post-training result with the baseline to demonstrate the effectiveness of the training.

IV. RESULTS

This section analyzes the results of the three experiments. Specifically, we analyze the system's transparency and force tracking performance, haptic feedback quality in palpation, and training benefits in suturing.

A. System Transparency Evaluation

Transparency is evaluated with position and force tracking RMSE/NRMSE errors from two users sharing control of two PSMs in free motion and contact. As shown in Table I, both operator consoles achieved sub-millimeter accuracy in position tracking, with all RMSE values below 0.2 mm. The corresponding NRMSE values were consistently below 1%, indicating highly accurate reproduction of the MTM trajectories at the PSM side. For force tracking, the RMSE values across all axes were below 1 N, and the NRMSE values remained under 10%, demonstrating reliable reflection of interaction forces. It is noteworthy that the errors along the z-axis were slightly higher than those along the x- and y-axes, which may be attributed to imperfect gravity compensation by the LSTM model. These results are comparable to dVRK bilateral teleoperation results in the literature [14], and confirm that the proposed multilateral teleoperation system provides high-fidelity position and force tracking. To complement these quantitative results, Fig. 8 provides position and force tracking plots from three consecutive contact motions along the x-y-z directions.

B. Haptic Feedback for Tumor Detection through Palpation

The performance of haptic feedback was evaluated through the palpation experiment where the users tried to determine hidden tumors in the phantoms. The success rate of the four tasks can be found in Table II.

As shown in Table II, the average accuracy of Tasks 1 and 2 was 83%, while that of Tasks 3 and 4 was 74%, indicating higher palpation accuracy in the single-operator case than in the dual-user case. This can be explained by the fact that when $\alpha = 1$, the environment force is fully transmitted to the operator. In contrast, when $\alpha = 0.5$, the environment force feedback is mixed with the other MTM force. Even if the second operator is not active, the added dynamics of the second MTM in the control loop induces operational force artifacts.

In addition, the average accuracy of Tasks 1 and 3 was 89%, whereas that of Tasks 2 and 4 was 68%, demonstrating that accuracy dropped substantially when the phantom condition changed from a large stiffness contrast to a small stiffness contrast. This is because the reduced stiffness contrast made the perceptual cues less distinguishable to the users. Overall, the system achieved an average accuracy of 78.5%, indicating that the multilateral teleoperation system can provide effective haptic feedback for stiffness discrimination.

TABLE II

ACCURACY OF TUMOR DETECTION THROUGH PALPATION

Task	α	**Phantom (Difficulty)**	**Success Rate (%)** Mean	(Min–Max)
1	1.0	Soft (Easy)	96.0	(80–100)
2	1.0	Firm (Hard)	70.0	(60–80)
3	0.5	Soft (Easy)	82.0	(60–100)
4	0.5	Firm (Hard)	66.0	(20–100)
Overall			78.5	(20–100)

C. Suturing Training Benefit

The training benefit was evaluated using the suture pulling experiment, and the effectiveness of training was assessed using two quantitative metrics: *Mean band error*, defined as the average deviation of the applied force from the target band [2.5, 4.5] N; and *In-band time*, defined as the percentage of time the applied force remained within the target band. To evaluate differences between baseline and post-training, paired t-tests were performed to capture changes within the subject.

As shown in Fig. 9, most participants demonstrated improved performance after training. Notably, four users broke the thread during the baseline trials, whereas no user experienced breakage after training, indicating the effectiveness of the proposed training framework. In terms of mean band error, nine out of ten users exhibited reductions, and the paired t-test yielded a statistically significant improvement ($p = 0.02$). This indicates that training effectively enhanced participants' ability to regulate the applied force within the desired range. For in-band time, nine users improved, and the paired t-test also showed a significant increase ($p = 0.02$), demonstrating that training helped participants to sustain their pulling force within the safety band for a longer duration. Importantly, these analyses excluded the trials with baseline breakage (NA values); therefore, the true training benefit is likely underestimated, as the complete elimination of breakage represents an additional and substantial improvement.

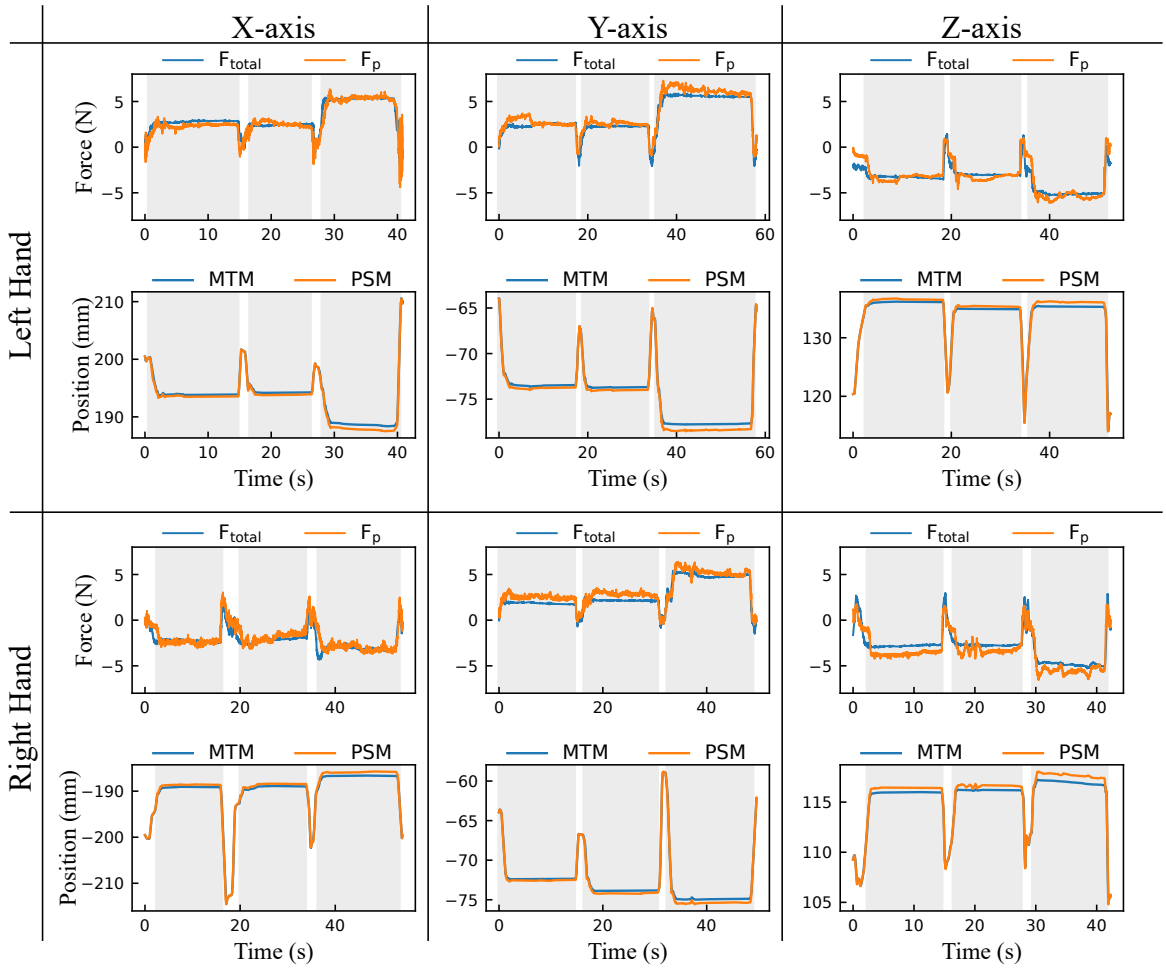

Fig. 8. Tracking performance of Force (N) and position trajectories (mm) between the MTMs and PSMs along the X, Y, and Z axes. Shaded regions represent contact with environment. $F_{total} = \alpha\hat{F}_E + (1-\alpha)\hat{F}_N$ and $F_p = -\gamma\hat{F}_P$, defined in eq. (6). $MTM = \alpha X_E + (1-\alpha)X_N$ and $PSM = \beta X_P$, which is defined in eq. (5). Position plots are for illustrative purposes only and are not summarized in Table I.

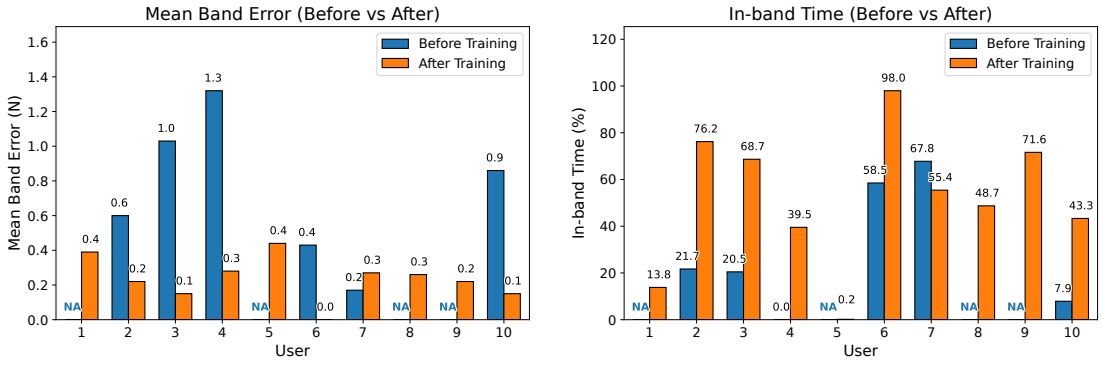

Fig. 9. Suturing force control performance metrics before and after training. NA indicates thread was broken in this trial.

V. CONCLUSIONS

This paper presents the first implementation of multilateral shared haptic control on a dual-console dVRK system. The system adopts a four-channel teleoperation architecture to achieve improved transparency, with a dominance factor introduced to change the training mode in accordance with the needs of surgical training tasks. Improved user performance after training with the system highlights the applicability

of the proposed system for surgical skill transfer. However, the user studies conducted have several limitations. The sample size was relatively small, and the results should be interpreted as preliminary validation. All participants were novices with non-medical backgrounds, so future studies with medical trainees and surgeons are needed for clinically relevant evaluation. In addition, while performance improved on immediate tasks, long-term skill retention and transfer with multilateral haptic guidance remain open questions.

The primary contribution of this paper is the first implementation and feasibility demonstration of multilateral shared haptic teleoperation on a dual-console dVRK, enabled by a four-channel architecture and learning-based force estimation. Accordingly, the present study focuses on system transparency characterization and pilot user studies to establish technical feasibility and training potential. Future work will include controlled comparisons against dual-console operation without haptic feedback to approximate current commercial mentoring workflows, as well as increasing controller bandwidth and incorporating dynamic compensation for enhanced tracking performance, integrating multisensory feedback such as visual overlays to better separate user and environment contributions, and conducting a discrete-time stability analysis to theoretically characterize the closed-loop stability of the proposed multilateral architecture.

REFERENCES

[1] R. H. Taylor, A. Menciassi, G. Fichtinger, P. Fiorini, and P. Dario, "Medical robotics and computer-integrated surgery," in *Springer Handbook of Robotics*. Springer, 2016, pp. 1657–1684.

[2] M. C. Moschovas, S. Saikali, A. Gamal, S. Reddy, T. Rogers, M. C. Sighinolfi, B. Rocco, and V. Patel, "First impressions of the new da Vinci 5 robotic platform and experience in performing robot-assisted radical prostatectomy," *European Urology Open Science*, vol. 69, pp. 1–4, 2024.

[3] A. M. Okamura, L. N. Verner, C. E. Reiley, and M. Mahvash, "Haptics for robot-assisted minimally invasive surgery," in *Robotics Research: The 13th International Symposium ISRR*. Springer, 2010, pp. 361–372.

[4] U. Hagn, R. Konietschke, A. Tobergte, M. Nickl, S. Jörg, B. Kübler, G. Passig, M. Gröger, F. Fröhlich, U. Seibold, L. Le-Tien, A. Albu-Schäffer, A. Nothhelfer, F. Hacker, M. Grebenstein, and G. Hirzinger, "DLR MiroSurge: a versatile system for research in endoscopic telesurgery," *Int. J. Comput. Assist. Radiol. Surg.*, vol. 5, no. 2, pp. 183–193, mar 2010.

[5] U. Kim, D.-H. Lee, W. J. Yoon, B. Hannaford, and H. R. Choi, "Force sensor integrated surgical forceps for minimally invasive robotic surgery," *Trans. Robot.*, vol. 31, no. 5, pp. 1214–1224, Oct 2015.

[6] R. Pena, M. J. Smith, N. P. Ontiveros, F. L. Hammond, and R. J. Wood, "Printing strain gauges on Intuitive Surgical da Vinci robot end effectors," in *IEEE/RSJ Int. Conf. Intell. Robots Syst.*, Oct 2018, pp. 806–812.

[7] Z. Chua and A. M. Okamura, "A modular 3-degrees-of-freedom force sensor for robot-assisted minimally invasive surgery research," *Sensors*, vol. 23, no. 11, p. 5230, 2023.

[8] A. Marban, V. Srinivasan, W. Samek, J. Fernández, and A. Casals, "A recurrent convolutional neural network approach for sensorless force estimation in robotic surgery," *Biomedical Signal Processing and Control*, vol. 50, pp. 134–150, 2019.

[9] Z. Chua, A. M. Jarc, and A. M. Okamura, "Toward force estimation in robot-assisted surgery using deep learning with vision and robot state," in *IEEE Int. Conf. Robot. Autom. (ICRA)*, 2021, pp. 12 335–12 341.

[10] N. Yilmaz, J. Y. Wu, P. Kazanzides, and U. Tumerdem, "Neural network based inverse dynamics identification and external force estimation on the da Vinci Research Kit," in *IEEE Int. Conf. Robot. Autom. (ICRA)*, 2020, pp. 1387–1393.

[11] B. Hannaford, "A design framework for teleoperators with kinesthetic feedback," *IEEE Trans. Rob. Auto.*, vol. 5, no. 4, pp. 426–434, 1989.

[12] D. A. Lawrence, "Stability and transparency in bilateral teleoperation," *IEEE Trans. Robot. Autom.*, vol. 9, no. 5, pp. 624–637, 1993.

[13] A. M. Okamura, "Methods for haptic feedback in teleoperated robot-assisted surgery." *Industrial Robot*, vol. 31, no. 6, pp. 499–508, 2004.

[14] N. Yilmaz, B. Burkhart, A. Deguet, P. Kazanzides, and U. Tumerdem, "Sensorless transparency optimized haptic teleoperation on the da Vinci Research Kit," *IEEE Robotics and Automation Letters*, vol. 9, no. 2, pp. 971–978, 2023.

[15] M. Beane, "Shadow learning: Building robotic surgical skill when approved means fail," *Administrative Science Quarterly*, vol. 64, no. 1, pp. 87–123, 2019.

[16] J. M. Albani and D. I. Lee, "Virtual reality-assisted robotic surgery simulation," *Journal of Endourology*, vol. 21, no. 3, pp. 285–287, 2007.

[17] A. Moglia, V. Ferrari, L. Morelli, M. Ferrari, F. Mosca, and A. Cuschieri, "A systematic review of virtual reality simulators for robot-assisted surgery," *European Urology*, vol. 69, no. 6, pp. 1065–1080, 2016.

[18] J. D. Bric, D. C. Lumbard, M. J. Frelich, and J. C. Gould, "Current state of virtual reality simulation in robotic surgery training: a review," *Surgical Endoscopy*, vol. 30, no. 6, pp. 2169–2178, 2016.

[19] J. Liu, S. Cramer, and D. Reinkensmeyer, "Learning to perform a new movement with robotic assistance: comparison of haptic guidance and visual demonstration," *Journal of Neuroengineering and Rehabilitation*, vol. 3, no. 1, p. 20, 2006.

[20] G. Rauter, R. Sigrist, R. Riener, and P. Wolf, "Learning of temporal and spatial movement aspects: A comparison of four types of haptic control and concurrent visual feedback," *IEEE Transactions on Haptics*, vol. 8, no. 4, pp. 421–433, 2015.

[21] A. E. Abdelaal, M. Sakr, A. Avinash, S. K. Mohammed, A. K. Bajwa, M. Sahni, S. Hor, S. Fels, and S. E. Salcudean, "Play me back: a unified training platform for robotic and laparoscopic surgery," *IEEE Robotics and Automation Letters*, vol. 4, no. 2, pp. 554–561, 2018.

[22] E. Fernandes, E. Elli, and P. Giulianotti, "The role of the dual console in robotic surgical training," *Surgery*, vol. 155, no. 1, pp. 1–4, 2014.

[23] S. Katsura and K. Ohnishi, "A realization of haptic training system by multilateral control," *IEEE Transactions on Industrial Electronics*, vol. 53, no. 6, pp. 1935–1942, 2006.

[24] B. Khademian and K. Hashtrudi-Zaad, "Performance issues in collaborative haptic training," in *IEEE International Conference on Robotics and Automation*. IEEE, 2007, pp. 3257–3262.

[25] ——, "Dual-user teleoperation systems: New multilateral shared control architecture and kinesthetic performance measures," *IEEE/ASME Transactions on Mechatronics*, vol. 17, no. 5, pp. 895–906, 2011.

[26] K. Shamaei, L. H. Kim, and A. M. Okamura, "Design and evaluation of a trilateral shared-control architecture for teleoperated training robots," in *2015 37th annual international conference of the IEEE engineering in medicine and biology society (EMBC)*. IEEE, 2015, pp. 4887–4893.

[27] U. Tumerdem and N. Yilmaz, "A unifying framework for transparency optimized controller design in multilateral teleoperation with time delays," *Control Engineering Practice*, vol. 117, p. 104931, 2021.

[28] A. Rashvand, M. Motaharifar, R. Heidari, A. Hassani, K. Hashtrudi-Zaad, M. Tavakoli, and H. D. Taghirad, "Robust control of collaborative dual-user haptic training system: An autonomous variable impedance scheme," *IEEE/ASME Transactions on Mechatronics*, 2024.

[29] P. Kazanzides, Z. Chen, A. Deguet, G. S. Fischer, R. H. Taylor, and S. P. DiMaio, "An open-source research kit for the da Vinci® Surgical System," in *IEEE Intl. Conf. on Robotics and Automation (ICRA)*. IEEE, 2014, pp. 6434–6439.

[30] N. Yilmaz, B. Burkhart, A. Deguet, P. Kazanzides, and U. Tumerdem, "Enhancing robotic telesurgery with sensorless haptic feedback," *International Journal of Computer Assisted Radiology and Surgery*, vol. 19, no. 6, pp. 1147–1155, 2024.

[31] W. Lear, L. L. Roybal, and J. J. Kruzic, "Forces on sutures when closing excisional wounds using the rule of halves," *Clinical Biomechanics*, vol. 72, pp. 161–163, Feb 2020.